Available online at www.sciencedirect.com
SCIENCE DIRECT®
Journal of Sound and Vibration 292 (2006) 179–202
JOURNAL OF SOUND AND VIBRATION
www.elsevier.com/locate/jsvi

Assessment of vibration-based damage identification techniques

A. Alvandi[a,*], C. Cremona[b]

[a]*Department of Civil Engineering, Université Laval, Québec (Québec), Canada G1K 7P4*
[b]*Laboratoire Central des Ponts et Chaussées, 58 Bd. Lefebvre, 75732 Paris, France*

Received 2 July 2004; received in revised form 6 July 2005; accepted 24 July 2005
Available online 26 September 2005

Abstract

In this paper some usual vibration-based damage identification techniques (VBDIT) will be reviewed and used for structural damage evaluation. With the help of a simple supported beam with different damage levels the reliability of these techniques will be investigated. The techniques reviewed herein are based on measured modal parameters which use only few mode shapes and/or modal frequencies of the structure that can be easily obtained by dynamic tests. In other words, by realizing two sets of dynamic measurements, corresponding to two moments of the structure lifetime, the dynamic modal parameters can be obtained. In order to assess properly the performance of these techniques different noise levels are randomly introduced to the response signals of a simulated beam which is exited by a random force. For different levels of damage and noise, the probabilities of damage detection and the probabilities of false alarm for the total number of simulations is evaluated. It can be concluded that among the evaluated techniques the strain energy method presents the best stability regarding noisy signals; however, the detection judgement depends on a threshold level which is discussed in this paper. The change in mode shape curvature, change in flexibility and change in flexibility curvature methods are also capable to detect and localise damaged elements but in the case of complex and simultaneous damages these techniques show less efficiency.

*Corresponding author. Tel.: +1 418 656 2131/5610; fax: +1 418 656 3355.
E-mail address: alireza.alvandi@gci.ulaval.ca (A. Alvandi).

0022-460X/$ - see front matter © 2005 Elsevier Ltd. All rights reserved.
doi:10.1016/j.jsv.2005.07.036

1. Introduction

Civil infrastructures begin to deteriorate once they are built and used. Maintaining safe and reliable civil infrastructure for daily use is a topic that has received considerable attention in the literature in recent years. Usual inspection techniques require the portion of the structure being inspected to be readily accessible and are therefore not appropriate due to interference with operational conditions. By definition, non-destructive techniques (NDT) are the means by which structures may be inspected without disruption or impairment of serviceability. Many methods have been developed for NDT, and an overview of the various techniques is presented by Witherell [1]. Some techniques are based on visual observations and some are based on the properties of the material. Other techniques are based on the interpretation of the structural condition by observing the change in the global behavior of the structure. The use of vibration test data to determine structural characteristics falls into this last category and are the subject of this paper.

The need of non-destructive and global techniques for structure diagnosis has led to the continuous development of methods examining the changes of dynamic characteristics. Such an approach has been introduced for several years in fields like automotive, aeronautical and mechanical engineering. The basic premise of the global damage detection methods that examine changes in the dynamic properties is that modal parameters, notably resonant frequencies, mode shapes, and modal damping, are a function of the physical properties of the structure (mass, damping, stiffness, and boundary conditions). Therefore, changes in physical properties of the structure, such as its stiffness or flexibility will cause changes in modal properties.

However, as any NDT, vibration-based damage identification techniques (VBDIT) are driven by many factors that can influence the result in the adequate decision as to the absence or presence of a damage. In general, any VBDIT comprises the application of a stimulus to a structure and the interpretation of the response to this stimulus. Repeated inspections of a specific damage will produce different response magnitudes of stimulus response because of minute variations in setup and calibration. This variability is inherent to the process. This is particularly the case when performing dynamic testing: the structural response is first recorded and then analyzed in order to extract, for instance, modal parameters. The data quality (signal-to-noise ratio) and the identification method can affect considerably the results regarding damage detection.

Mazurek [2], Doebling and Farrar [3] are the pioneers in examining the statistical significance of damage identification results. This statistical significance was studied via application to the data from tests performed on the Interstate 40 highway bridge in Albuquerque, New Mexico. Since then, different aspects of these methods have been investigated on the bases of experimental results mostly obtained from existing bridges [4,5]. It is the intent of this paper to explore further the issue of the statistical significance of the changes for a particular damage indicator. The approach demonstrated in this paper uses random noise simulations to compute probabilities of damage detection and probabilities of false alarm. These probabilities allow to estimate performance qualification of a VBDIT.

2. Vibration-based damage identification techniques (VBDIT): a review

In this section, the current VBDIT which are validated by a number of experimental results [4,5] will be reviewed. As in practical damage evaluation it would be always difficult to excite the

structural high modal frequencies (need of high quantity of energy), all selected techniques requiring few mode shapes and/or modal frequencies. These methods do not require an analytical model of the structure, only some modal frequencies and mode shapes, before and after damage are necessary which can be obtained by dynamic tests.

2.1. Mode shape curvature method

In formulating the eigenvalue problem, Pandey et al. [6] assumed that structural damage only affects the stiffness matrix and not the mass matrix. For the undamaged condition the eigenvalue problem is expressed as

$$([K]-\lambda_i[M])\{\Phi_i\}=\{0\}, \tag{1}$$

where $[K]$ and $[M]$ are, respectively, the stiffness and mass matrices, λ_i and $\{\Phi_i\}$ are the ith eigenvalue and the ith eigenvector. Similarly, the eigenvalue problem for the damaged condition is

$$([K^*]-\lambda_i^*[M])[\Phi_i^*]=\{0\}, \tag{2}$$

where the asterisks identify the stiffness matrix, the ith eigenvalue and the ith eigenvector of the damaged structure. The pre- and post-damage eigenvectors are the basis for damage detection. Mode shape curvature for the beam in the undamaged and damaged condition can then be estimated numerically from the displacement mode shapes.

Given the undamaged and damaged mode shapes, consider a beam cross section at location x subjected to a bending moment $M(x)$. The curvature at location x, $v''(x)$, is given by

$$v''(x)=\frac{M(x)}{EI}, \tag{3}$$

where E is the modulus of elasticity and I the moment of area of the section. Thus, for a given moment applied to the damaged and undamaged structure, a reduction of stiffness associated with damage will, in turn, lead to an increase in curvature. Furthermore, an estimation of the extent of damage can be obtained by measuring the amount of change in the mode shapes curvatures.

2.2. Change in flexibility method

Another class of damage identification methods uses the dynamically measured flexibility matrix to estimate changes in the static behavior of the structure [7]. Because the flexibility matrix is defined as the inverse of the static stiffness matrix, the flexibility matrix F relates the applied static force f and resulting structural displacement u as

$$\{u\}=[F]\{f\}. \tag{4}$$

The expression of the flexibility matrix is written as

$$[F]=[\Phi][\Omega]^{-1}[\Phi]^{\mathrm{T}}=\sum_{i=1}^{n}\frac{1}{\omega_i^2}\{\Phi_i\}\{\Phi_i\}^{\mathrm{T}}, \tag{5}$$

$[\Phi]=[\{\Phi_1\},\{\Phi_2\},\ldots,\{\Phi_n\}]$ is the mode shapes matrix, $\{\Phi_i\}$ being the ith mode shape. The diagonal matrix of rigidity $[\Omega]$ correspond to $[\omega_i^2]$, where ω_i is the ith frequency. $[F]$ is finally the flexibility matrix. Thus, each column of the flexibility matrix represents the displacement pattern of the

structure associated with a unit force applied at the associated degree of freedom. Measuring the flexibility matrices before and after damage, the variation matrix $[\Delta]$ can be obtained:

$$[\Delta] = [F^*] - [F], \tag{6}$$

where $[F]$ and $[F^*]$ are, respectively, flexibility matrices before and after damage. Now, for each column of matrix Δ, let $\bar{\delta}_j$ be the absolute maximum value of the elements in the jth column. Hence,

$$\bar{\delta}_j = \max|\delta_{ij}|, \quad i = 1, \ldots, n, \tag{7}$$

where δ_{ij} are elements of matrix Δ and represent the flexibility variation in each degree of freedom. The column of the flexibility matrix corresponding to the largest $\bar{\delta}_j$ is indicative of the degree of freedom where the maximum variation in flexibility has been produced or the location of the damage.

2.3. Change in flexibility curvature method

By combining certain aspects of the mode shape curvature method and the change in flexibility method, Zhang and Aktan [8] developed an alternative damage detection scheme. Similarly to the mode shape curvature method, the basic concept is that a localized loss of stiffness will produce a curvature increase at the same location. However, the change in curvature is obtained from the flexibility instead of the mode shapes.

The flexibility matrices, before and after damage can be approximated by the modal parameters:

$$[F] = [\{F_1\}\{F_2\}\cdots\{F_n\}] \approx [\Phi][\Omega]^{-1}[\Phi]^{\mathrm{T}} \tag{8}$$

and

$$[F^*] = [\{F_1^*\}\{F_2^*\}\cdots\{F_n^*\}] \approx [\Phi^*][\Omega^*]^{-1}[\Phi^*]^{\mathrm{T}}, \tag{9}$$

where the asterisks designate the damaged structure. F_1 through F_n (with and without the asterisk) correspond to columns of the flexibility matrix. Zhang and Aktan used the change in curvature of the flexibility matrix to determine the location of damage. The curvature change is evaluated as follows:

$$[\Delta] = \sum_{i=1}^{n} |\{F_i^*\}'' - \{F_i\}''|, \tag{10}$$

where $[\Delta]$ and n represent, respectively, the absolute curvature change and the number of degrees of freedom (or identified number of mode shapes).

2.4. Strain energy method

Considering a three-dimensional beam of the type Bernoulli–Euler of length L (Fig. 1), the strain energy can be expressed as [9]

$$U = \frac{1}{2}\int_0^L \left[\mathrm{EI}_z(x)\left(\frac{\partial^2 v}{\partial x^2}\right)^2 + \mathrm{EI}_y(x)\left(\frac{\partial^2 w}{\partial x^2}\right)^2 + \mathrm{EA}(x)\left(\frac{\partial u}{\partial x}\right)^2 + \mathrm{GJ}_x(x)\left(\frac{\partial \psi_x}{\partial x}\right)^2 \right] \mathrm{d}x, \tag{11}$$

where u, v, w are, respectively, the displacements in the x, y, z directions and ψ_x is a rotational displacement about x-axis. EI_z, EI_y represent, respectively, the flexural rigidities about z and y axes and EA, GJ_x are the longitudinal and the torsional rigidities.

The starting point of the strain energy method is the formulation of the strain energy of a Bernoulli–Euler beam. In this investigation only the flexural rigidity about z-axis (first expression of Eq. (11)) will be considered, this approach can be generalized to the three-dimensional beam-like structures and the plate-like structures [4] which are beyond the scope of this paper. The next paragraphs resume some essential elements of the method [10]:

Considering just the first expression of Eq. (11), for a beam of length L the strain energy can be simplified as

$$U = \frac{1}{2}\int_0^L EI_z(x)\left(\frac{\partial^2 y}{\partial x^2}\right)^2 dx. \tag{12}$$

From now on for simplicity, EI_z will be replaced by EI. If a mode shape ϕ_i is considered, the associated strain energy is given by

$$U_i = \frac{1}{2}\int_0^L EI(x)\left(\frac{\partial^2 \phi_i}{\partial x^2}\right)^2 dx. \tag{13}$$

Assuming that the beam is divided in N elements, the strain energy by element for a given mode shape may therefore be expressed by

$$U_{ij} = \frac{1}{2}\int_{a_j}^{a_{j+1}} EI(x)\left(\frac{\partial^2 \phi_i}{\partial x^2}\right)^2 dx \tag{14}$$

with a_j, a_{j+1} delimiting the element j. From the strain energy related to each element and the strain energy of the complete structure for a given mode, the fractional strain energy F_{ij} which is the ratio between the element strain energy and the beam strain energy can be defined [10]:

$$F_{ij} = U_{ij}/U_i \tag{15}$$

with $\sum_{j=1}^{N} F_{ij} = 1$, where N is the number of elements.

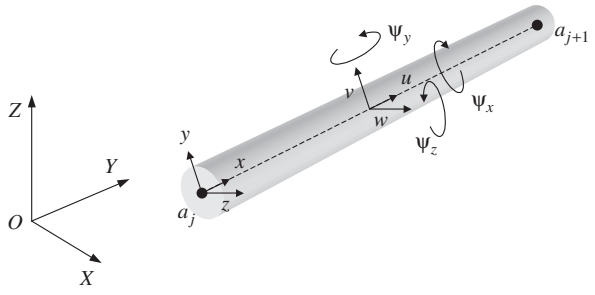

Fig. 1. Three-dimensional beam element.

Similar expressions can be derived for a damaged case:

$$F_{ij}^{*} = U_{ij}^{*}/U_{i}^{*}; \quad U_{i}^{*} = \frac{1}{2}\int_{0}^{L} \mathrm{EI}^{*}(x)\left(\frac{\partial^2 \phi_i^{*}}{\partial x^2}\right)^2 \mathrm{d}x,$$

$$U_{ij}^{*} = \frac{1}{2}\int_{a_j}^{a_{j+1}} \mathrm{EI}^{*}(x)\left(\frac{\partial^2 \phi_i^{*}}{\partial x^2}\right)^2 \mathrm{d}x. \tag{16}$$

In presence of small damages, a first-order approximation can be drawn:

$$F_{ij}^{*} = F_{ij} + \text{higher-order terms} \tag{17}$$

leading to

$$1 = \frac{F_{ij}^{*}}{F_{ij}} = \frac{U_{ij}^{*}U_i}{U_{ij}U_i^{*}} = \frac{\int_{a_j}^{a_{j+1}} \mathrm{EI}^{*}(x)(\partial^2\phi_i^{*}/\partial x^2)^2\,\mathrm{d}x}{\int_{a_j}^{a_{j+1}} \mathrm{EI}(x)(\partial^2\phi_i/\partial x^2)^2\,\mathrm{d}x}\,\frac{\int_0^L \mathrm{EI}(x)(\partial^2\phi_i/\partial x^2)^2\,\mathrm{d}x}{\int_0^L \mathrm{EI}^{*}(x)(\partial^2\phi_i^{*}/\partial x^2)^2\,\mathrm{d}x}. \tag{18}$$

Using the generalized mean value theorem:

$$\exists \hat{x} \in [a,b] \int_a^b f(u)g(u)\,\mathrm{d}u = f(\hat{x})\int_a^b g(u)\,\mathrm{d}u, \tag{19}$$

when f is continuous and g non-negative and integrable, it becomes

$$1 = \frac{\widehat{\mathrm{EI}}_j^{*}\int_{a_j}^{a_{j+1}}(\partial^2\phi_i^{*}/\partial x^2)^2\,\mathrm{d}x}{\widehat{\mathrm{EI}}_j\int_{a_j}^{a_{j+1}}(\partial^2\phi_i/\partial x^2)^2\,\mathrm{d}x}\,\frac{\widehat{\mathrm{EI}}^{*}\int_0^L(\partial^2\phi_i/\partial x^2)^2\,\mathrm{d}x}{\widehat{\mathrm{EI}}\int_0^L(\partial^2\phi_i^{*}/\partial x^2)^2\,\mathrm{d}x}. \tag{20}$$

Assuming that EI is essentially constant over the length of the beam for both the undamaged and damaged modes ($\widehat{\mathrm{EI}}^{*} \approx \widehat{\mathrm{EI}}$), Eq. (20) can be rearranged to give an indication of the change in flexural rigidity of the damaged element:

$$\frac{\widehat{\mathrm{EI}}_j}{\widehat{\mathrm{EI}}_j^{*}} = \frac{\int_{a_j}^{a_{j+1}}(\partial^2\phi_i^{*}/\partial x^2)^2\,\mathrm{d}x}{\int_{a_j}^{a_{j+1}}(\partial^2\phi_i/\partial x^2)^2\,\mathrm{d}x}\,\frac{\int_0^L(\partial^2\phi_i/\partial x^2)^2\,\mathrm{d}x}{\int_0^L(\partial^2\phi_i^{*}/\partial x^2)^2\,\mathrm{d}x}. \tag{21}$$

The right-term of Eq. (21) is independent of the mode shape: by taking the mean of a set of n mode shapes, this equation can be rewritten as

$$\beta_j = \frac{\widehat{\mathrm{EI}}_j}{\widehat{\mathrm{EI}}_j^{*}} = \frac{1}{n}\sum_{i=1}^{n}\frac{\int_{a_j}^{a_{j+1}}(\partial^2\phi_i^{*}/\partial x^2)^2\,\mathrm{d}x}{\int_{a_j}^{a_{j+1}}(\partial^2\phi_i/\partial x^2)^2\,\mathrm{d}x}\,\frac{\int_0^L(\partial^2\phi_i/\partial x^2)^2\,\mathrm{d}x}{\int_0^L(\partial^2\phi_i^{*}/\partial x^2)^2\,\mathrm{d}x}. \tag{22}$$

This expression slightly differs from the one introduced in [10]. β_j is the damage index for element j. In order to generalize damage index independently of the structure type, a normalized damage index is often preferred and may be expressed as

$$z_j = (\beta_j - \bar{\beta})/\sigma_\beta, \tag{23}$$

where $\bar{\beta}, \sigma_\beta$ are the mean and standard deviations of the sample values β_j. This normalization leads to negative values for undamaged elements and positive ones for potential damaged

locations. However, the question arises how to classify a positive value of z_j as a damaged and undamaged elements.

2.4.1. Classification criterion

In this paper, the probabilities of detection and false alarm will be used to determine the number of positive or negative calls. As an outcome example a beam with four damaged locations is considered. The normalized damage index z_j obtained from a strain energy method is shown in Fig. 2.

The negative indexes are related to undamaged cases and the positive indexes identify a potentially damaged element, the main task is selecting an adequate threshold level (z_j) in order to define the real damaged elements. This threshold level can be considered as a discriminating level. If this acceptance criterion is placed at a too high level ($z_j = 1.5$), some damages will be unrevealed. At a proper level ($z_j = 1$), clear discrimination will result. If the acceptance criterion is too low ($z_j = 0.5$), several false alarms will result. Therefore, an adequate level must be determined allowing clear discrimination. Several techniques can be applied and the most classical one is to introduce a statistical pattern recognition based on the Neyman–Pearson test [10]. This requires some statistical assumptions (normality) which are difficult to validate. Another option used in this paper is based on the concepts of probabilities of detection and false alarm [11]. As it will be shown later, many parameters such as noises and damage locations can have an important influence on these probabilities.

3. Principle of study and noise simulation

In order to study the performance of the presented VBDIT regarding different factors that can have an influence on detection results, a model of a continuous beam was selected as the test

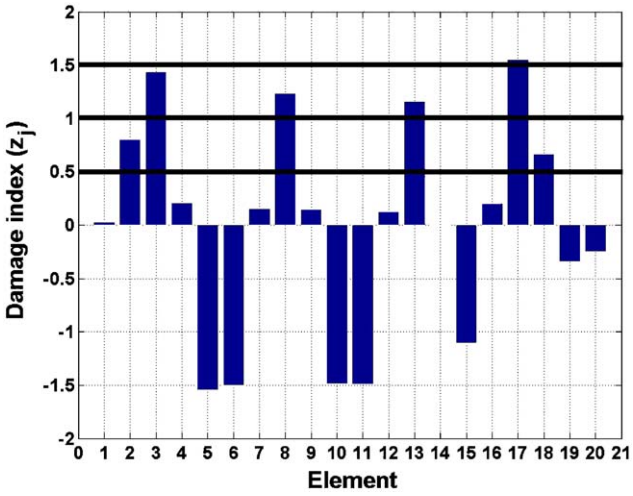

Fig. 2. Example of damage index distribution and threshold level influence (damaged elements: 3%, 8%, 13%, 17% with 2% reduction in stiffness).

model. The model consisted of 20 elements (2 nodes linear elements with 3 degree of freedom per node); for better demonstration the elements are presented in two dimensions (Fig. 3). Values for the material properties of the beam elements were assigned as follows: (1) the elastic modulus $E = 21.1\,\text{MPa}$; (2) the linear mass density $\rho = 798.1\,\text{kg/m}^3$. Values for the geometric properties were assigned as follows: (1) the cross-sectional area $A = 0.02\,\text{m}^2$ and the moment of area $I = 666.7 \times 10^{-8}\,\text{m}^4$. Applying a random force, a linear dynamic analysis was performed and the signals at each nodal point were measured. The analysis time was 15 s with the sampling time of 0.002 s.

Different levels of damage (1%, 2%, 4%, 6%, 8%, 10% reduction of the rigidity of an element) were introduced on one or two elements. After initial investigations, it was determined that an additional 3% noise level could be considered as a high level of noise. The corresponding noise levels which were added to the measurement signals were considered as follows: 0.1–0.25–0.5–0.75–1–1.5–2–2.5–3% signal/noise. For each noise simulation, the percentage of noise was multiplied to the standard deviation value of each measuring channel and it was randomly added to other component of current channel (multiplying to random numbers between −1 and 1). The noisy signals (before and after damage) were treated by the random decrement technique [12] which was developed under Matlab© [13]. The triggering condition in this technique was positive point and the sampling time was 0.002 s.

A total of 250 simulations were generated. In other words, 250 series of modal parameters before and after damage were obtained. After signal treatment the identified modal parameters were used as an entrance data for the presented VBDIT. The three first identified frequencies were 5.88, 23.52 and 52.2 Hz and the corresponding mode shapes used for damage evaluation are given in Fig. 4. Before going on, the signification of detection and false alarm probabilities will be presented in the following paragraphs.

4. Probabilities of detection and false alarm

The mode shape curvature, change in flexibility and change in flexibility curvature methods present the quantity of variation in each degree of freedom, so the degree of freedom which presents the maximum variation will identify the location of damage. In contrast with the other techniques the strain energy method does not provide the absolute value of variation, therefore as

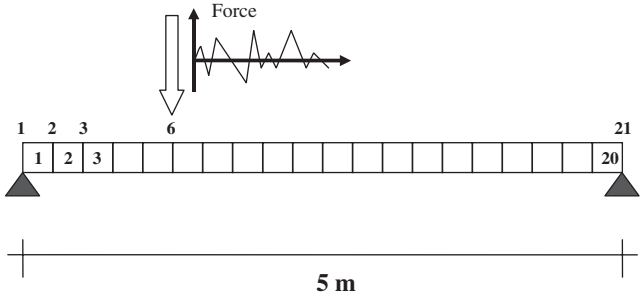

Fig. 3. Test model, random force applied on the simple supported beam.

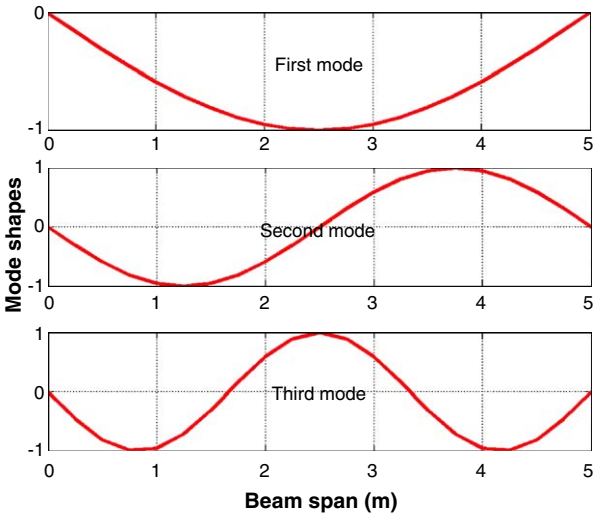

Fig. 4. Mode shapes used for damage evaluation.

mentioned before, it is necessary to introduce the concept of threshold level. A damage is detected if the normalized indicator takes a value superior to this threshold level. The objective is to find out how this threshold level can be defined in presence of the different noise levels.

For the mode shape curvature, change in flexibility and change in flexibility curvature methods, if n_s represents the number of simulated noisy response for a given level of noise and n_d the number of realisations that an actual damage is detected, the percentage of detection probability will be given by

$$P_d = \frac{n_d}{n_s} \times 100. \tag{24}$$

The probability of false alarm will be given by complementary probability of detection:

$$P_f = 100 - P_d. \tag{25}$$

For the strain energy method, the numbers of realisations that the real damage is detected is function of the retained threshold detection level z_s:

$$P_d = \frac{n_d(z_s)}{n_s} \times 100 \tag{26}$$

and in this case the probability of false alarm is not the complementary of the probability of detection. If n_f represents the number of times that existing damage is not being detected (that means $z_j \leqslant z_s$, j indicates an element of the mesh), then the percentage of false alarm probability is given by

$$P_f = \frac{n_f}{n_s} \times 100. \tag{27}$$

For n_s simulations, the procedure of detection and false alarm probabilities related to presented VBDIT is given in Fig. 5.

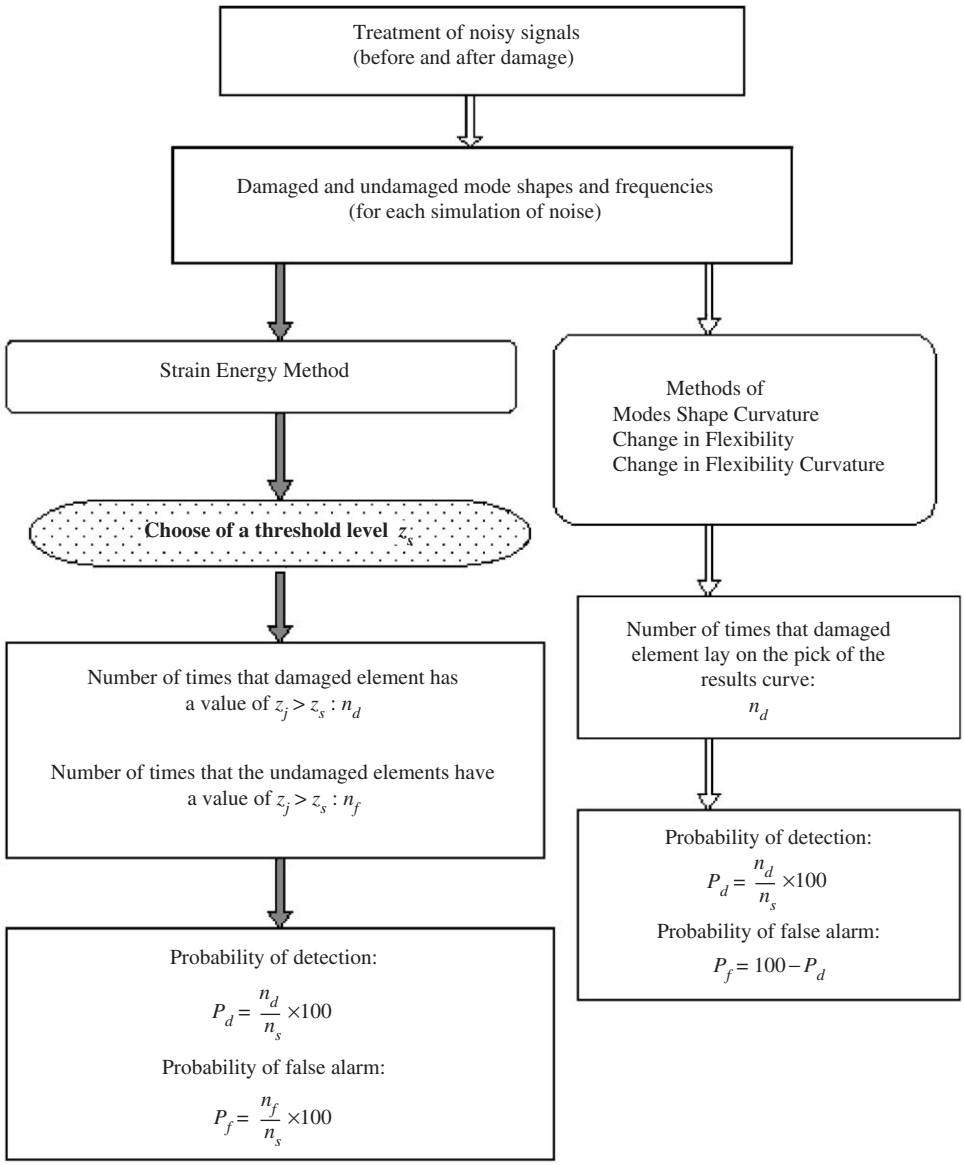

Fig. 5. Calculation process of detection and false alarm probabilities.

5. Study procedure

A random force for a period of 40 s (Fig. 6) was applied to node 6 of the presented beam (Fig. 3). To study the influence of the damaged element location in comparison with the force application point, several damaged elements located at different sections along the beam length were considered. Afterwards, the case of simultaneous damaged elements was considered. As presented methods are based on few numbers of mode shapes and/or modal frequencies, in the

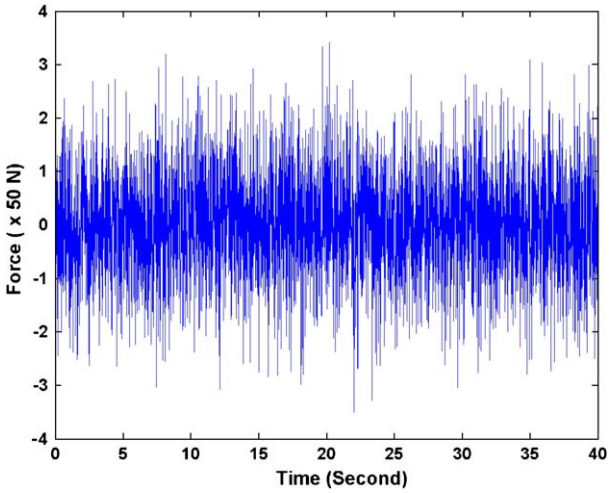

Fig. 6. Random force of excitation.

carried out simulation, only the three first mode shapes and modal frequencies have been considered. Fig. 7, for 5% of rigidity lost and various levels of noise, presents an outline of the means (rectangular bars) and plus/minus one standard deviation (solid circles) values of damage indicator (z_s) for 250 simulated mode shapes. Fig. 7 shows that by increasing noise level the mean values of simulation results on damage element decrease and the results become more dispersing.

6. Simulation results for one damaged element

6.1. Damaged element far from the source of excitation

Element 11, located near the mid-span of the beam and therefore at a far distance from the point of excitation is first considered as a damaged element (Fig. 3). The probabilities of detection (P_d) and false alarm (P_f), provided by the strain energy method for three threshold level ($z = 2; z = 1.5; z = 1$) are shown in Fig. 8. As we discussed, the results are functions of the selected threshold level; by decreasing the threshold level the probability of detection and false alarm increase. Considering the detection probabilities shown in Fig. 8, it is evident that for all the three used threshold levels ($z = 2; z = 1.5; z = 1$), by increasing the level of damage (light to dark colored cubic bars) the probabilities of detection increase and by increasing the noise level (0.1–3%) the probabilities of detection decrease. As shown in Fig. 8, the false detection probabilities are depending on the selected threshold levels. In fact, the objective is to select an adequate threshold level in order to have a maximum probability of detection and a minimum probability of false alarm.

For comparison purposes Fig. 9 shows the probability of damage detection for the three other methods for the same damaged element (element 11). According to these results, the change in flexibility (Fig. 9b) and change in flexibility curvature (Fig. 9c) methods for 0.1% of noise provide almost 100% of detection probabilities for the damaged element. Among these three techniques

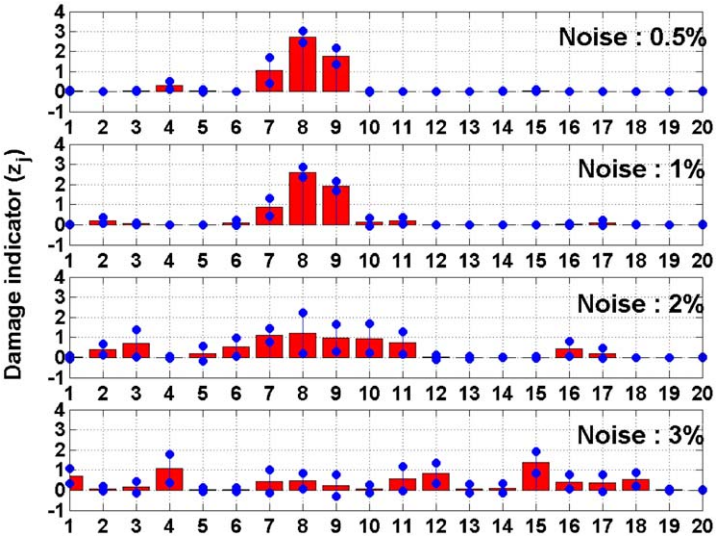

Fig. 7. Dispersion of damage indicator (damaged element: 8, stiffness reduction: 5%).

the results obtained from the mode shape curvature method are less efficient than the other methods. In the next section, the disadvantage of each one of these three methods regarding the damage location and simultaneous damages will be discussed.

The other preoccupation concerning the VBDIT is the accuracy of these methods regarding the damage zone; in other words how precisely they can detect damage locations. To highlight this effect Figs. 10 and 11 give the probabilities of detection and false alarm by considering two neighboring elements (elements 9 and 12). In this case the detection criteria is based on detecting one of three elements (elements 9, 10 and 12) as a damaged element. In the case of the strain energy method (Fig. 10), in comparison to Fig. 8 for the same threshold levels, the probabilities of false alarm show an important decrease and the probabilities of detection show an increase. The false alarm reduction signifies that the majority of the false detections are due to the neighboring elements. As expected the same observation can be drawn from Fig. 11; in comparison to Fig. 9, the probabilities of detection of all the three presented methods show an increase, this would be more evident in the case of the change in flexibility method in Fig. 11b, in comparison to Fig. 9b.

6.2. *Damaged element located close to the excitation source*

To evaluate the effect of the excitation location on the evaluating results, element 5, which was located close to the excitation source, was considered as a damaged element (Fig. 3). The probabilities of detection obtained by the strain energy method are shown in Fig. 12. Comparing Fig. 12 to the detection probabilities obtained from the previous case with the same threshold levels, where the damage element was located far from the excitation source (Fig. 8), it would be evident that location of the excitation point does not have an important influence on the results of the strain energy method. Furthermore comparison between Figs. 13 and 9, clearly shows that the other methods expressed much more difficulty in detecting the damaged element when this is

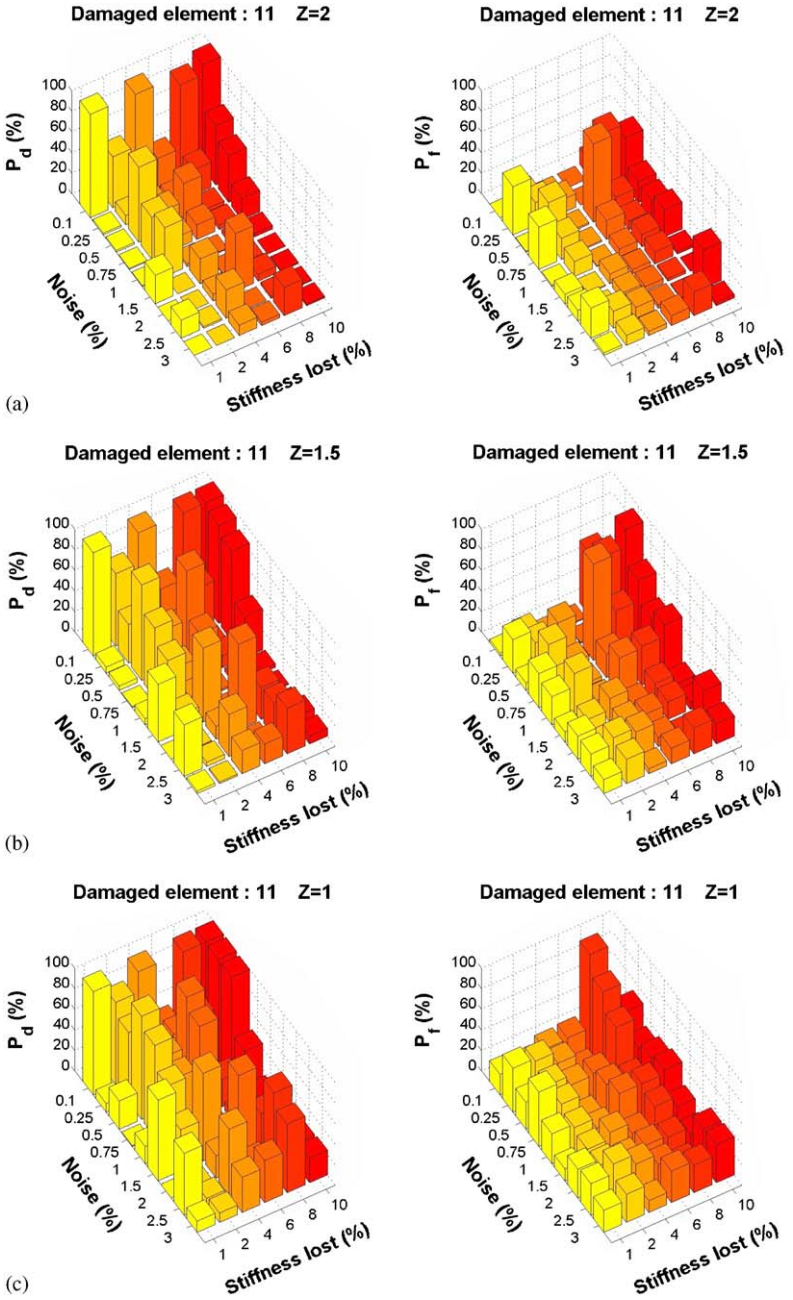

Fig. 8. Probability of detection (P_d) and false alarm (P_f) of the strain energy method for a damaged element located far from source of excitation: (a) $Z = 2$; (b) $Z = 1.5$; (c) $Z = 1$.

located near the excitation force: change in flexibility method (Fig. 13b), provides almost no detection while the mode shape curvature method (Fig. 13a), for a high level of damage (more than 4% of rigidity lost) and a very low level of noise (less than 0.75%), provides a low percentage

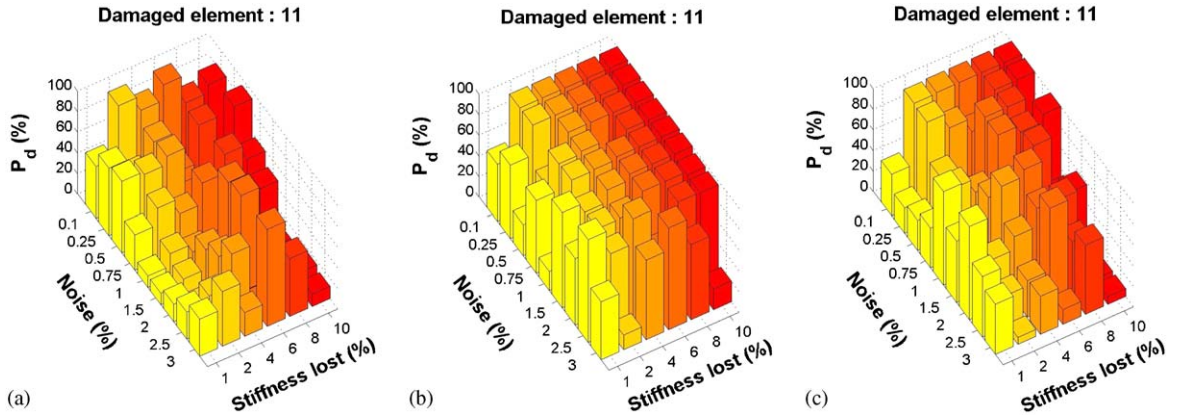

Fig. 9. Probability of detection (P_d) for a damaged element located far from source of excitation: (a) mode shape curvature; (b) change in flexibility; (c) change in flexibility curvature methods.

of detection probabilities. Finally, the change in flexibility curvature method (Fig. 13c), provides better detection than the other methods for damages greater than 4%.

6.3. Damaged element near to a support

As previous simulated and experimental results obtained by the presented VBDIT show, it has always been a difficult task to detect damages located near the supports [4]. This situation may be due to false detections which often cause at these locations. To verify the influence of the noise on damage evaluation of the elements located near the supports, element 2 was considered as a damaged element (Fig. 3). Fig. 14 presents the strain energy results for the same threshold level as the previous cases. In order to increase the probability of detection for certain levels of noise and damage, the threshold level must be reduced to 1 or even less than 1 which has the inconvenience to rise the false alarm probabilities (lost of detection quality). As was presented before, the majority of these false detections are due to the neighboring element. According to Fig. 15, when the strain energy method may reach a P_d of more than 80% for certain levels of noise and damage, the other methods are totally inappropriate and incapable of any damage detection.

7. Simulation results for two damaged elements

In order to evaluate noise effect on the results of the simultaneous damaged elements, two scenarios of damage were considered; first the two damaged elements were positioned relatively far from the supports and the excitation point and in the second, one of these damaged elements were located near a support. The following paragraphs present the details of these scenarios.

7.1. Damaged elements far from source of excitation

Two elements relatively far from the excitation point and the supports were considered (Fig. 16). Fig. 17 presents the probabilities of detection and false alarm provided by the strain

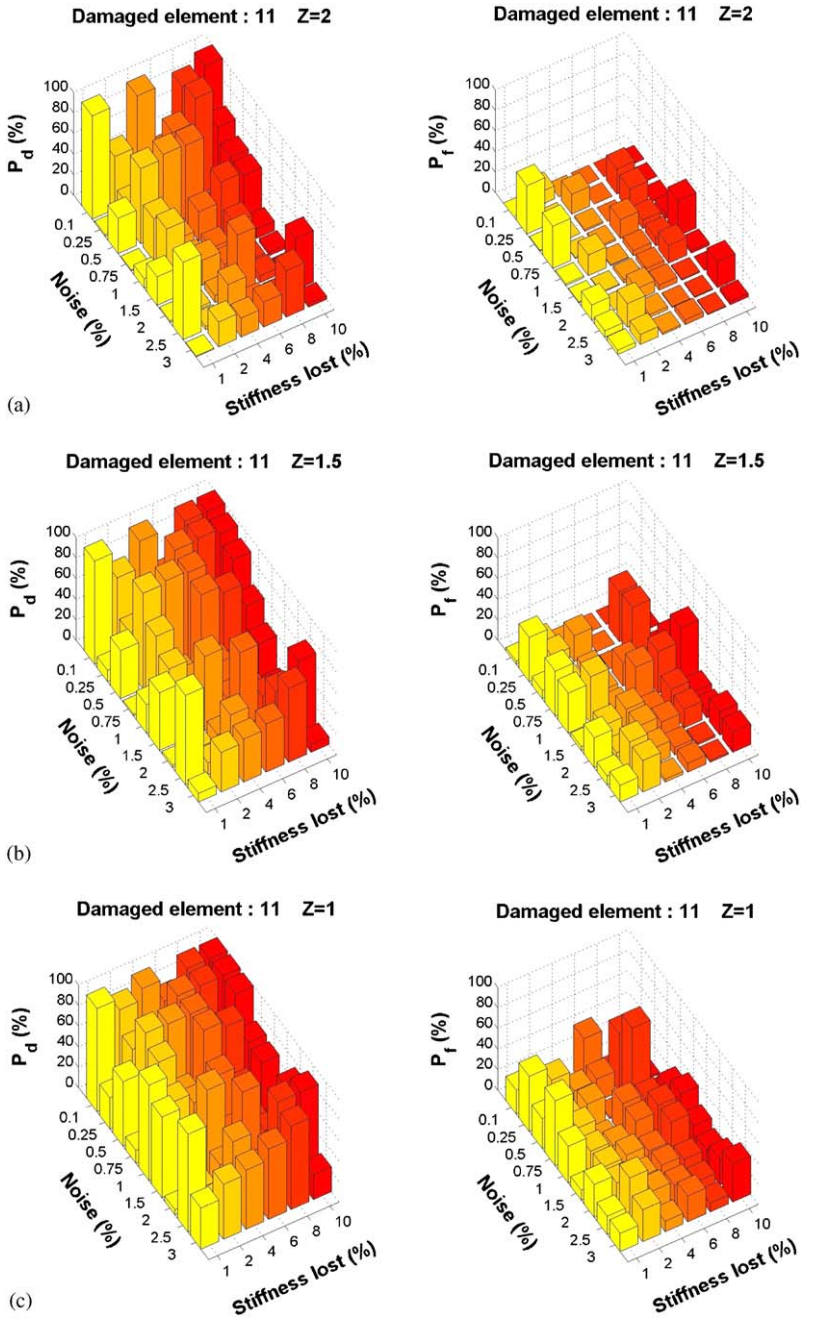

Fig. 10. Probability of detection (P_d) and false alarm (P_f) of the strain energy method, considering the neighboring elements of a damaged element located far from source of excitation: (a) $Z = 2$; (b) $Z = 1.5$; (c) $Z = 1$.

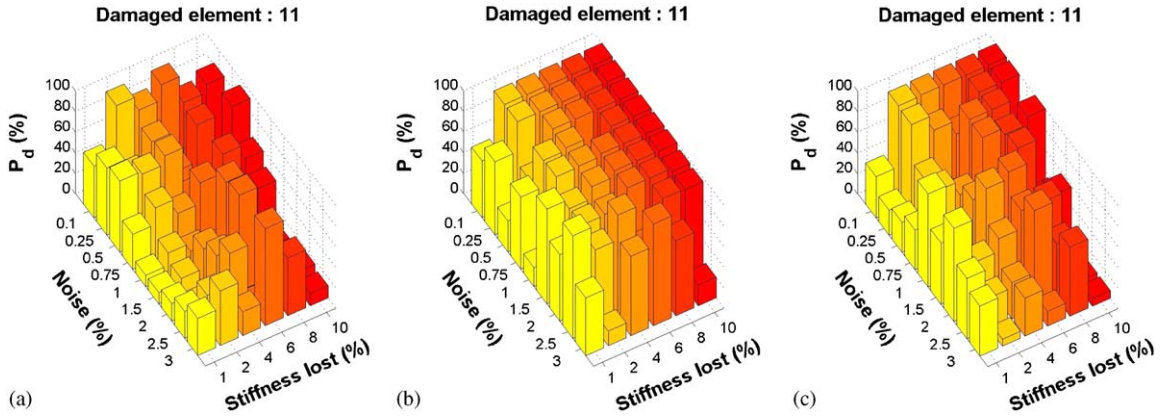

Fig. 11. Probability of detection (P_d), considering the neighboring elements of a damaged element located far from source of excitation: (a) mode shape curvature, (b) change in flexibility; (c) change in flexibility curvature methods.

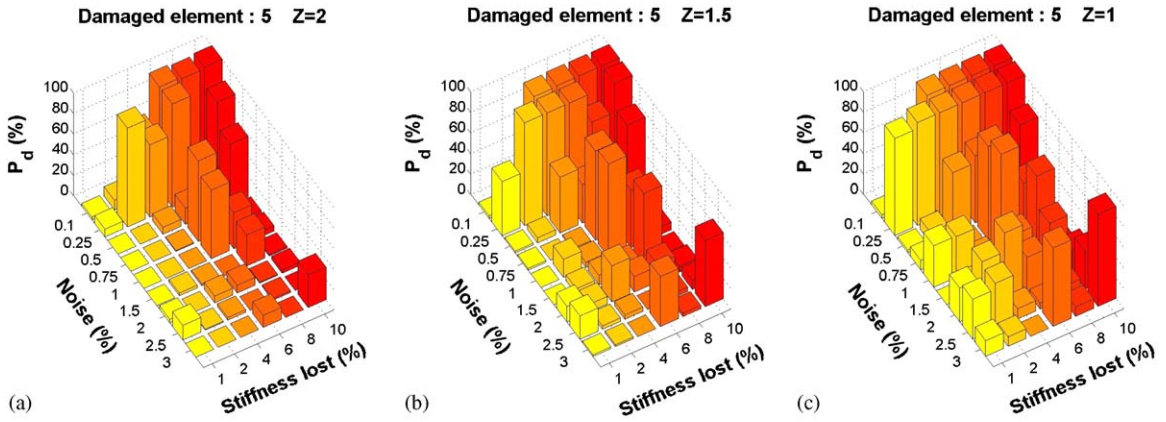

Fig. 12. Probability of detection (P_d) of the strain energy method for a damaged element located close to the excitation source: (a) $Z = 2$; (b) $Z = 1.5$; (c) $Z = 1$.

energy method. In this case, in order to be able to localise damaged elements the threshold levels were reduced to 1.8 and 1. As Fig. 17 shows, reducing the threshold level to $z_j = 1$ would provide better equilibrium between the detection and false alarm probabilities. As shown in Fig. 17, in either case ($z = 1.8; z = 1$) the probabilities of detection for the second damaged element (17) are less than the first one (9). The detection probabilities of the other methods are given in Fig. 18. The probabilities provided by the change in flexibility (Fig. 18b) and change in flexibility curvature (Fig. 18c) methods are more accurate than the change in curvature method (Fig. 18a). Concerning the second damaged element, except a few detection for very low level of noise; less than 0.25% (Fig. 18c), these three methods are almost incapable to detect damaged element.

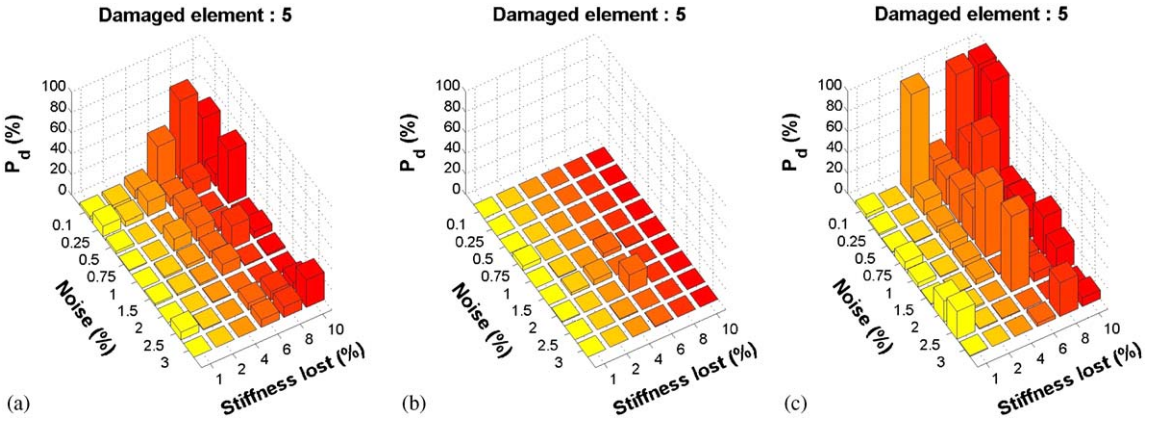

Fig. 13. Probability of detection (P_d), considering the neighboring elements of a damaged element located close to the excitation source: (a) mode shape curvature, (b) change in flexibility, (c) change in flexibility curvature methods.

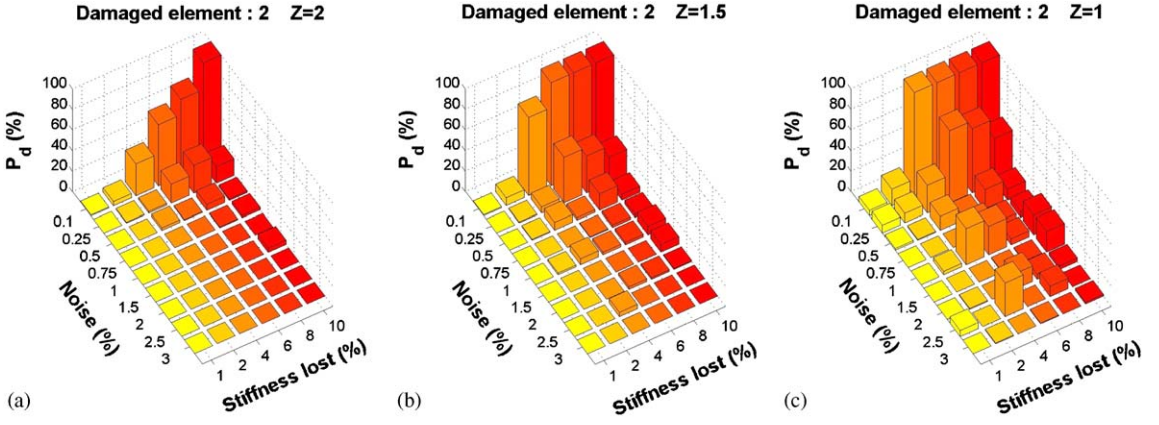

Fig. 14. Probability of detection (P_d) of the strain energy method for a damaged element located near to a support: (a) $Z = 2$; (b) $Z = 1.5$; (c) $Z = 1$.

7.2. *Presence of an element close to a support*

To highlight the effect of supports in presence of two damaged elements, one of the damaged elements was situated near a support (Fig. 19). The probabilities obtained from strain energy method for these two elements (2 and 17) are shown in Fig. 20. In this scenario, in contrast with the previous cases, the previous threshold levels ($z = 2$; $z = 1.5$) did not provide much damage detection, so in order to increase the detection probabilities for different levels of noise and damage the threshold level was reduced to 1 and 0.5. Fig. 21 presents the detection probabilities obtained from other methods. Except for the change in flexibility curvature method which provided some detection for the second damage element (Fig. 21c), the other methods were incapable to detect damaged elements.

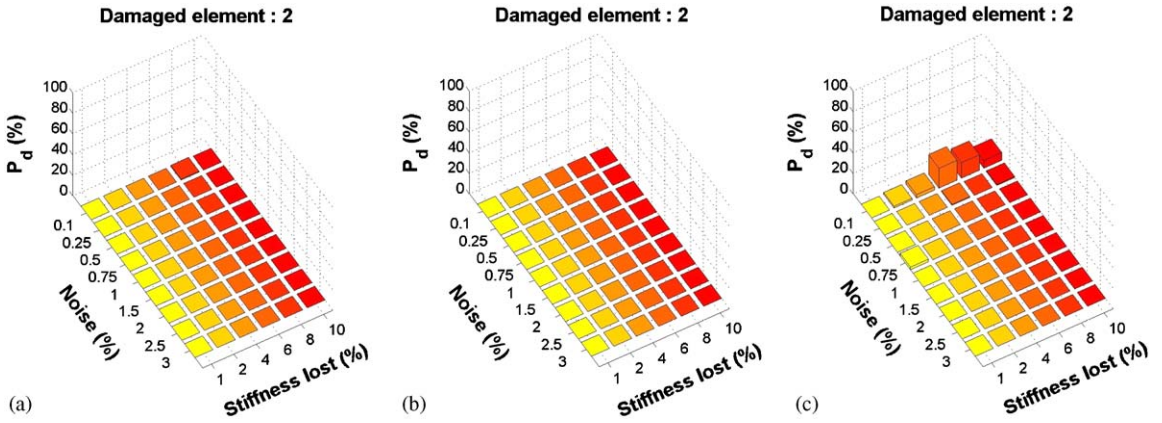

Fig. 15. Probability of detection (P_d) for a damaged element located near to a support: (a) mode shape curvature, (b) change in flexibility, (c) change in flexibility curvature methods.

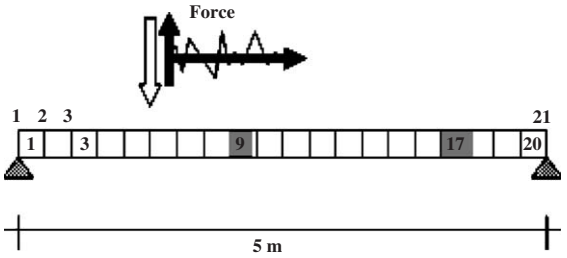

Fig. 16. Beam with the damaged elements 9 and 17, far from excitation source.

8. Conclusions

The purpose of the present paper has been to illustrate how practically used VBDIT would behave in presence of variability in modal parameters which are often inevitable. As the sources of this variation are often unknown, noise simulations were introduced as a first approach to the problem. Different levels of noise were added to the response signals of a simple supported beam and the modal parameters of the noisy signals were identified. Applying VBDIT to identified modal parameters with different levels of noise and damage the following conclusions can be obtained:

- According to the simulation results (Figs. 8, 12, 14, 17, 20), the strain energy method presents the best stability regarding the noisy signals. Knowing that the detection results are completely dependent on the selected threshold level and that classification level might be modified according to the location and nature of damages.
- The effect of the neighboring elements, which introduces many false alarm detections, enables the strain energy method to reduce the threshold level in order to detect the

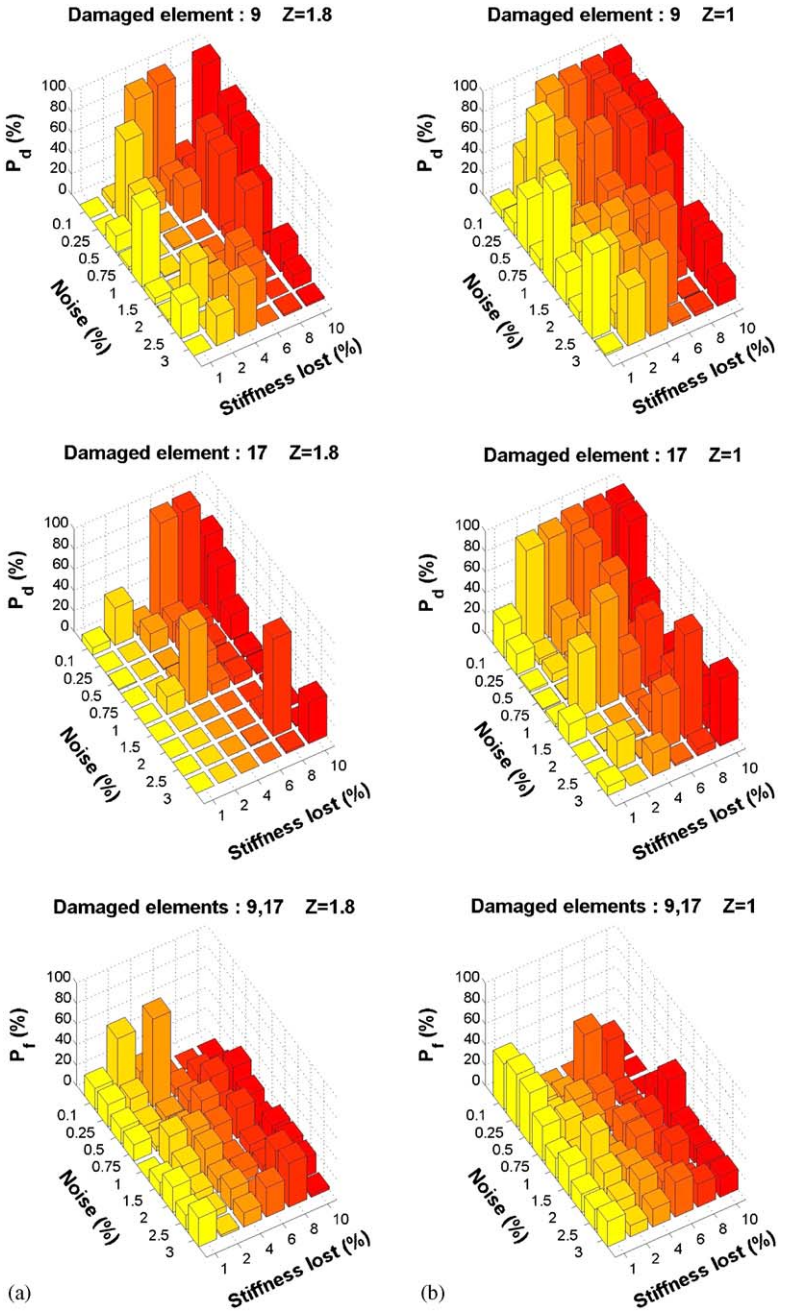

Fig. 17. Probability of detection (P_d) and false alarm (P_f) of the strain energy method for two damaged elements far from excitation source: (a) $Z = 1.8$; (b) $Z = 1$.

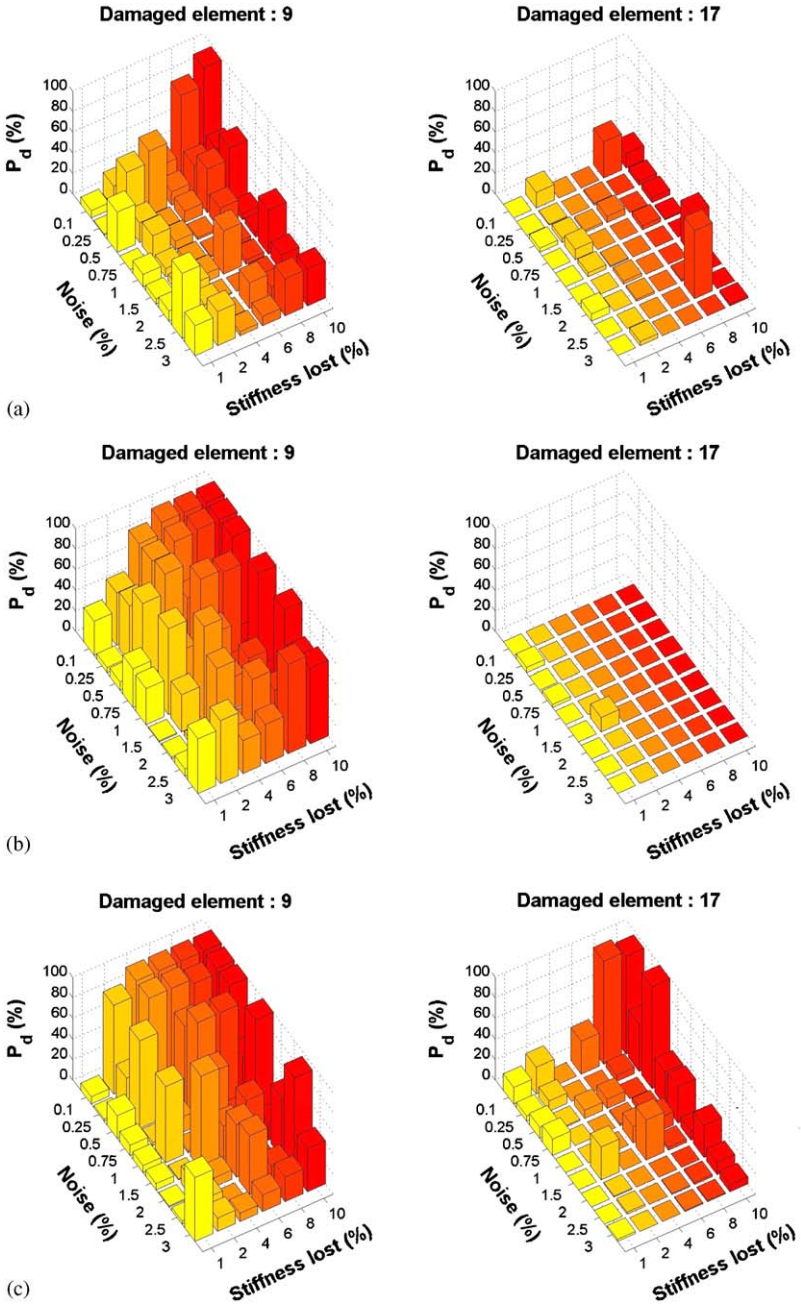

Fig. 18. Probability of detection (P_d) for two damaged elements far from excitation source: (a) Mode shape curvature, (b) change in flexibility, (c) change in flexibility curvature methods.

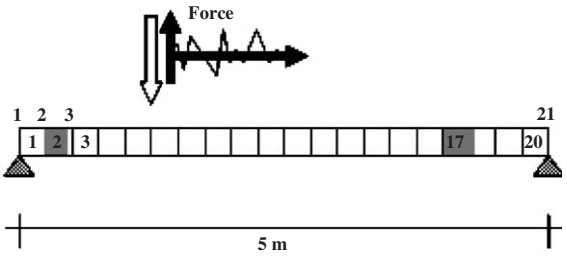

Fig. 19. Beam with the damaged elements 2 and 17.

difficult located damages (example, reducing the threshold levels to 1 and 0.5 in Fig. 20).

- In the case of two damaged elements far from the excitation source, all presented methods have difficulties in detecting the element which locates close to supports; by reducing the threshold level, the strain energy method is easily able to detect this second damaged element.
- As the strain energy method uses the normalised damaged index (z_j), this threshold level approach is general and independent of the type of the structure. This feature makes this method a global powerful tool for health monitoring of different structures.
- The results of many experimental research [14,15] show that a thermal fluctuation can be considered as an important factor in modal identification processes and can have an effect especially on frequencies. As strain energy method uses only few number of mode shapes (not the frequency), it would behave much better than the other VBDIT.
- As the strain energy method does not provide the quantity of damage, but the probability of being damaged element in the detected location, it is necessary to compare the detection results with the other quantitative methods as presented in this investigation.
- The three other presented methods (change in mode shape curvature, change in flexibility and change in flexibility curvature) are also able to quantify the damages elements, but in the complex and simultaneous damage cases they are less efficient.
- Regarding the boundaries effect, using the presented methods together can reduce detection error; even though especial attention must be paid in these areas.

The experimental data of the existing structures; Interstate 40 highway bridge in Albuquerque, New Mexico [4], Z24 Bridge in Switzerland [4], A High Speed Railway Bridge in France [16], Saint Marcel Bridge in Canada [5],… evaluated by authors using the presented methods, show that, in the complex case of simultaneous damages, damages close to the supports (or joints) or in the case of low quality of registered data, the strain energy and flexibility curvature methods both together are quite adequate for detecting the structural modifications. Regarding strain energy method, choosing the threshold level between 1.5 and 2 provide quite satisfactory results [4].

Current investigation was the first approach to the noise effect on the VBDIT and it was realised on a simple supported beam. In order to generalize the threshold level approach based on the strain energy method, the effect of noise on more sophisticated structures need to be studied.

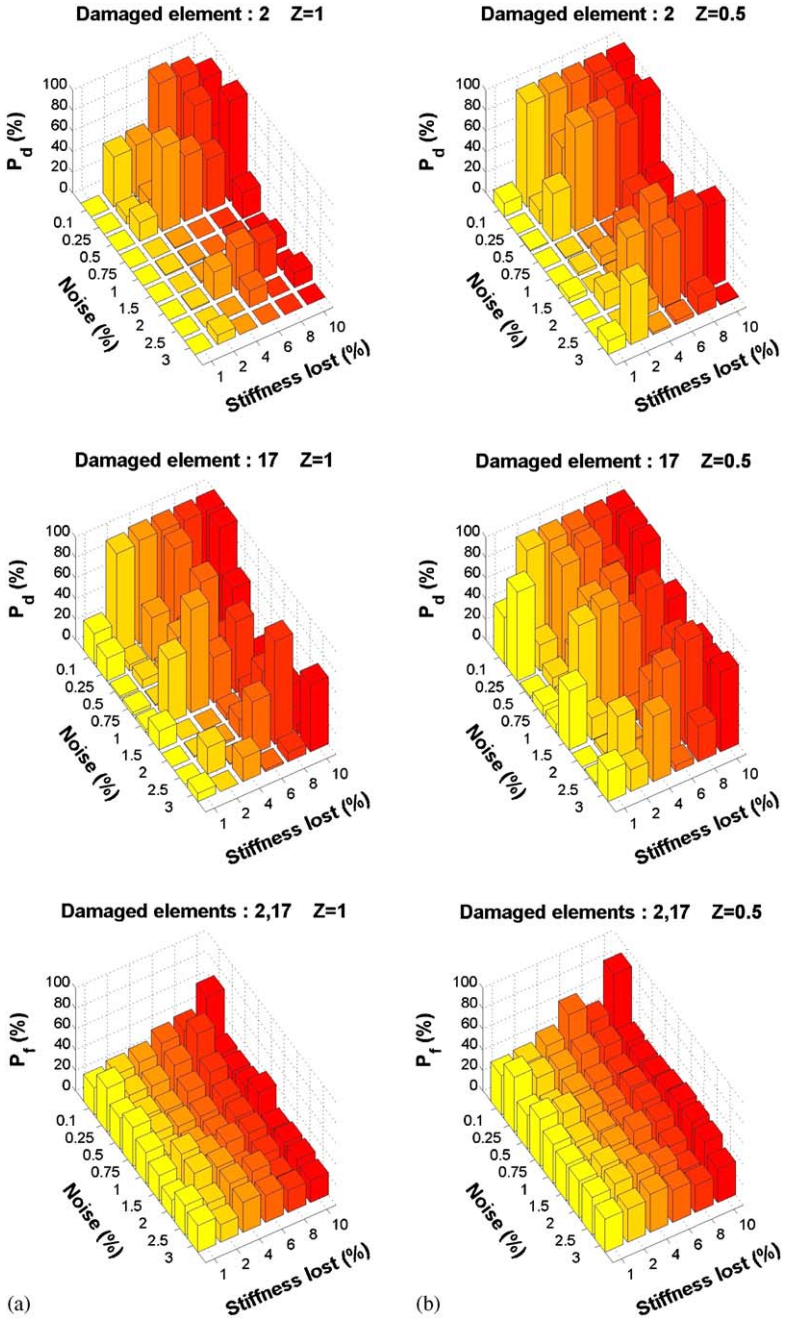

Fig. 20. Probability of detection (P_d) and false alarm (P_f) of the strain energy method for two damaged elements, one close to a support: (a) $Z = 1$; (b) $Z = 0.5$.

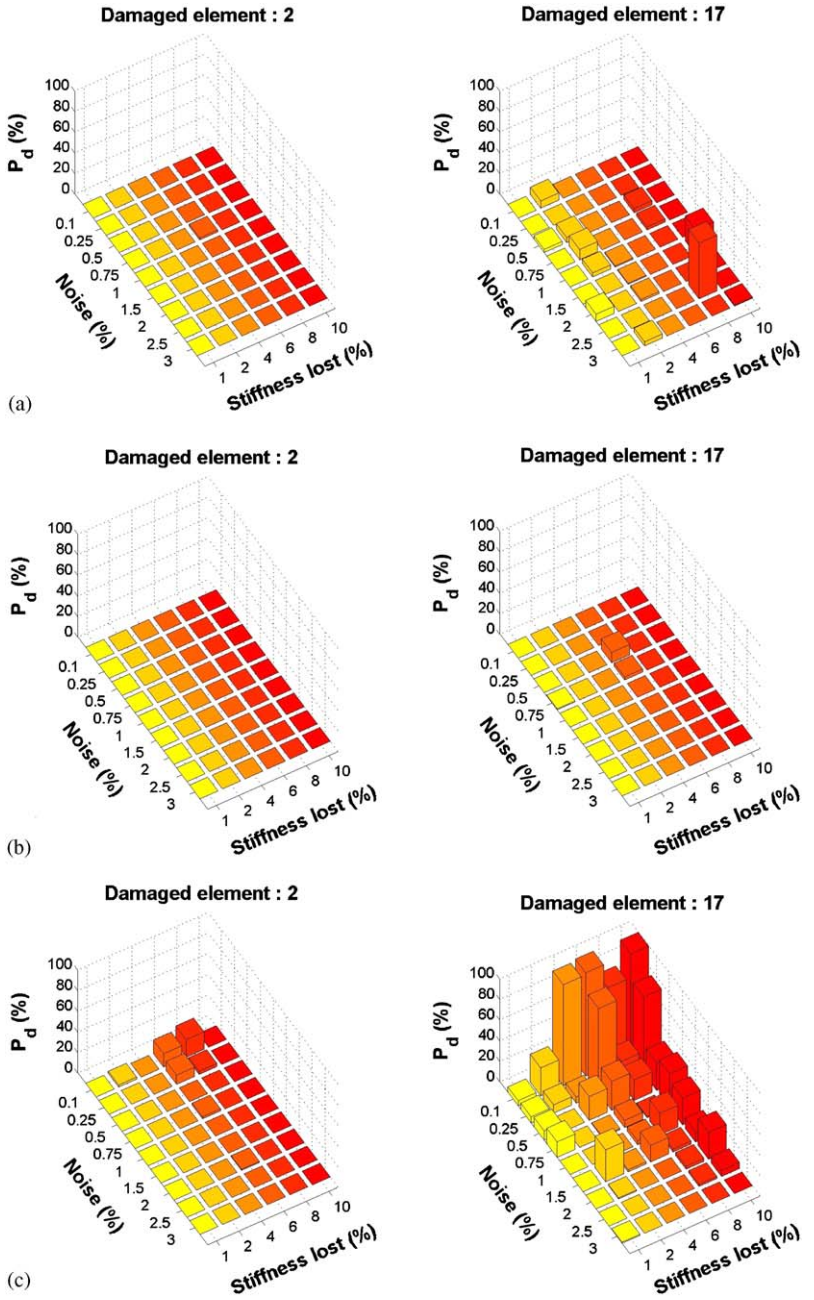

Fig. 21. Probability of detection (P_d) for two damaged elements, one close to a support: (a) Mode shape curvature, (b) change in flexibility, (c) change in flexibility curvature methods.

References

[1] C.E. Witherell, *Mechanical Failure Avoidance: Strategies and Techniques*, McGraw-Hill, New York, 1994.

[2] D.F. Mazurek, Modal sensitivity to damage in multigirder bridges, in: *Proceedings of the IMAC*, vol. 15, 1997, pp. 1898–1982.
[3] S.W. Doebling, C.F. Farrar, Statistical damage identification techniques applied to the I-40 bridge over the Rio Grande River, in: *Proceedings of the IMAC*, vol. 16, 1998, pp. 1717–1724.
[4] A. Alvandi, Contribution à l'utilisation pratique de l'évaluation dynamique pour la détection d'endommagements dans les ponts. Ph.D. thesis, École Nationale des Ponts et Chausses, 2003.
[5] A. Alvandi, J. Bastien, C. Cremona, M. Jolin, Évaluation d'endommagement par essais dynamiques, izème colloque sur la progression de la recherche québécoise sur les ouvrages d'art, Université Laval, Quebec, Canada, 2005.
[6] A.K. Pandey, M. Biswas, M.M. Samman, Damage detection from changes in curvature mode shapes, *Journal of Sound and Vibration* 145 (2) (1991) 321–332.
[7] A.K. Pandey, M. Biswas, Damage detection in structures using changes in flexibility, *Journal of Sound and Vibration* 169 (1) (1994) 3–17.
[8] Z. Zhang, A.E. Aktan, The damage indices for constructed facilities, in: *Proceedings of the IMAC*, vol. 13, 1995, pp. 1520–1529.
[9] M. Géradin, D. Rixen, *Mechanical Vibrations: Theory and Application to Structural Dynamics*, second ed., Wiley, New York, 1997.
[10] P.J. Cornwell, S.W. Doebling, C.R. Farrar, Application of the strain energy damage detection method to plate-like structures, *Journal of Sound and Vibration* 224 (2) (1999) 359–374.
[11] A. Alvandi, C. Cremona, Reliability of bridge integrity assessment by dynamic testing, in: *Proceedings of the First European Structural Health Monitoring Conference*, 2002, pp. 125–137.
[12] J.C. Asmussen, Modal analysis based on the random decrement technique—applications to civil engineering structures, Ph.D. Thesis, Aalborg University, 1997.
[13] F.S. Barbosa, Cremona C. Identification modal de structures sous solicitation ambiante. *Final Report*, Laboratoire Central des Ponts et Chausses (LCPC), vol. 1&2, 2002.
[14] M.A. Waheb, G. De Roeck, Effect of temperature on dynamic system parameters of a highway bridge, *Structural Engineering International* 4/97 (1997) 266–270.
[15] C.R. Farrar, S.W. Doebling, P.J. Cornwell, E.G. Straser, Variability of modal parameters measured on the Alamosa Canyon bridge, in: *Proceedings of the IMAC*, vol. 15, 1997, pp. 257–263.
[16] C. Cremona, P. Hallak, A. Alvandi, D. Ducret, M.H. Inchauspé, L. Dieleman, Dynamic monitoring of a high speed railway bridge, in: *Proceedings of the Second International Conference on Bridge Maintenance*, Safety and Management (IABMAS'04), Kyoto, Japan, 2004, pp. 233–234.